

Designing a Low-Cost Early Diagnosis System Based on Deep Learning

Monitoring the Development of Chronic Venous Disorder with Indirect Augmented Reality

Huseyin A. Erdem

Department of Computer Engineering,
The Graduate School of Natural and
Applied Sciences
Dokuz Eylül University
İzmir, Turkey
e-mail: huseyinaerdem@gmail.com

Hışıl Erdem

Department of Civil Engineering,
The Graduate School
İzmir Institute of Technology
İzmir, Turkey
e-mail: isilerdem@iyte.edu.tr

Semih Utku

Department of Computer Engineering,
Faculty of Engineering
Dokuz Eylül University
İzmir, Turkey
e-mail: semih@cs.deu.edu.tr

Abstract - Today's healthcare industry agrees that early diagnosis is just as important as the treatment of diseases. Academic and commercial studies carried out in this direction within the scope of early diagnosis contribute to a better quality of human life. Thanks to devices that offer early diagnosis, treatments can be started when the diseases are at their initial levels, and thus treatment costs can be reduced. However, most of these devices work with harmful rays and are generally used in hospital environments only by specialized staff. In this study, a low-cost early diagnosis system for home use, developed as part of a doctoral thesis, is introduced. The most important aspect of the proposed system that supports the convenience of home use is that it provides a harmless imaging with near-infrared light for the body. The system can detect both Class-1 (spider/telangiectasias vein) and Class-2 (varicose vein) types of the clinical classification of Chronic Venous Disorder, with 4 different classes (in the form of two separate levels as beginner and advanced). In the system, which will monitor the development of the disorders in the superficial veins, the confidence values and positions of the detections in the images were determined by the You Only Look Once version-3 object detection algorithm used in deep learning applications. Confidence values of 0.90 and above were achieved in the object detection experiments performed with Class-1 and Class-2 type artificial patterns. According to the test results obtained, the system was able to detect Chronic Venous Disorder patterns with the values of Accuracy Rate (1), Misclassification Rate (0), Precision (1), Prevalence (0.5) and F-Score (1). The confidence values and positions of the patterns detected in the study are presented to the user/physician with the help of indirect augmented reality visuals as an e-health application that will support a long-term monitoring system. In this way, the beginner and the advanced levels of venous disorder can be monitored by before and after video visuals.

Keywords - near-infrared light; chronic venous disorder; deep learning; YOLOv3; indirect augmented reality.

I. INTRODUCTION

Especially in the 21st century, in the academic and commercial sector, advances in health technologies have increased at an unstoppable pace. While some of these advances target treatments after the disease occurs, others aim at early diagnosis by making use of various imaging

techniques that are harmful/harmless to the body. This study is an extended version of the study [1] investigating the detection of varicose vein development. In this version, the current system designed for vascular degeneration monitoring within the scope of the doctoral thesis [2] has been restructured in such a way that it can detect 2 different types (spider_vein and varicose_vein) of vein enlargement at 2 levels (beginner and advanced) in more detail. The current system [2] consists of 6-phases. In the Imaging Technique Phase, video recordings of superficial veins are obtained using a low-cost (65 dollars) near-infrared camera. With the Digital Image Pre-Processing Phase, these recordings are converted into images and enhancements are made on the raw images. These first two phases are detailed in the study [3]. In the enhanced images, the discontinuous vascular structures caused by illumination are removed to a certain level in the Digital Image Post-Processing Phase. In the Classification Phase, the classes of vascular degeneration are determined by using Convolutional Neural Networks and Hybrid Decision-Making Algorithm (first introduced in the study [4]), and the positions of these degenerations are determined in the Object Detection Phase. In the last phase, the Augmented Reality Phase, the object detection results obtained are superimposed on the raw images, and the video visuals are created and presented to the user and his/her physician. All phases of this system are described in the study [4] specifically for vascular narrowing (stenosis_vein class).

Medical imaging devices are one of the primary auxiliary methods used in hospitals to diagnose different diseases. The devices used in this context work on the basis of visualizing the area to be viewed with light or sound waves. Imaging with light is carried out by utilizing different wavelengths in the electromagnetic spectrum. Medical imaging devices currently in use are classified according to “the body tissue they can monitor” and “the effects of the light used to illuminate the area of interest on the body”. While the X-Ray device, which emits harmful rays (ionizing radiation) to the body, is predominantly used in the imaging of bone tissue and abdominal diseases, Computed Tomography is used for imaging both bone tissue and internal organs [5]-[7]. In addition, Magnetic Resonance Imaging provides imaging of tissues with magnetic waves, whereas Ultrasound uses high-

frequency sound waves for imaging [5][6]. Computed Tomography or Magnetic Resonance Imaging techniques can be used for vascular imaging [6]. However, both the negative effects of these devices on human health and their high costs limit their use to hospital environments only. Furthermore, even if the ultrasound device, which provides visualization of blood flow [5][6], is harmless to the body, it has a high cost and is generally used and interpreted by radiologists in hospitals.

Although technology advances at a dizzying pace, many lives are still lost due to late detection of diseases that can be easily cured if detected earlier. Despite efforts to raise awareness of early diagnosis of all kinds of diseases, today's people do not give up the habit of going to the doctor after the onset of the disease and often neglect routine checkups. In these omissions, the concern of triggering other diseases by imaging devices working with harmful rays to the body during controls has a large share. However, technological techniques currently under development offer the possibility of producing safe alternatives for the early detection of some diseases. Among them, we can include, the detection of varicose veins, which is one of the most common venous disorders and caused by the enlargement of veins close to the surface of the skin (i.e., superficial veins), can be counted. Near-infrared light, which is a type of light that is harmless to the body, is used in hospitals within the scope of superficial vein imaging, especially during vascular access procedures.

The main advantage of near-infrared light in the scope of vein imaging is that photons of this type of light can be absorbed by Hemoglobin molecules in the veins [8]-[10]. The Hemoglobin (Hb) molecule is a blood protein [11] that is found in the vascular system and is in charge of carrying Oxygen to the tissues. While the molecule carries Oxygen to the tissues and organs by passing through the arteries in the form of oxygenated Hb (HbO_2), it returns to the heart through the veins as de-oxygenated Hb (Hb) after leaving its Oxygen. These molecules transported in a recirculation system are more sensitive to near-infrared light in the range of 800-900 nanometers (nm) as HbO_2 and in the range of 700-800 nm as Hb [12]. One of the tricks in near-infrared imaging is to choose the wavelength of the near-infrared light that illuminates the tissue and the wavelength of the camera that will take the image in harmony. In this way, the veins in the tissue area illuminated with near-infrared light of a certain wavelength (in the studies carried out in [9]-[13], a wavelength of 850 nm was used, which usually gives optimum results) can be viewed in a better quality with a camera having the same wavelength filter. Superficial veins (thanks to the Hb molecules inside) absorb the near-infrared light (700-900 nm range of the electromagnetic spectrum) that penetrates 3-5 millimeters, passing through the skin and fat layer in the illuminated tissue area, and creates dark areas in the images. These dark areas in the images represent the veins, while the bright areas represent the surrounding tissues. In this way, the visualization of the superficial veins can be easily performed with only the light source and the camera (even an ordinary camera can be turned into a simple near-infrared camera by changing the filter on it). This

imaging method is evaluated within the scope of Spectroscopy (acquiring knowledge of the structure of matter interacting with a particular type of light [14]). Although the dark areas in near-infrared spectroscopy images more or less allow the visualization of veins, they are not of sufficient quality for further analysis. For this, by applying digital image processing filters on the obtained near-infrared image, some improvements can be made on the image. The 6-phase system used in the study performs image enhancement processes in two separate phases. In the Digital Image Pre-Processing Phase, two-coloured binary images consisting of black (vein) and white (surrounding tissues) are obtained from raw videos (video recordings are taken during tissue imaging) with image processing filters and methods. In this way, it is ensured that the edges of the veins are sharpened, only the relevant vein patterns are revealed by eliminating the surrounding tissues and the noise in the images is removed. In the veins of these images, the discontinuous structures caused by the illumination have been eliminated up to a certain level with the Digital Image Post-Processing Phase (Speeded Up Robust Features (SURF) Local Feature Detector Algorithm [15] is used). Processed near-infrared vascular images can be used for many different purposes from disease pre-diagnosis to biometric recognition [3][4][16][17]. For these purposes, deep learning techniques (such as classification or object detection/recognition) are applied on images. The Classification Phase of the 6-phase system makes it possible to determine to which class the observed tissue belongs. At this phase, video recordings of the first viewing period are used to introduce the classes to be used in the system. Within the scope of monitoring, the system checks the belongingness of the images obtained in the following periods (can be set as day, week, month) to one of the defined classes (as many as the number of different tissue regions the user views in the first period). If the classes of new images can be determined, the Object Detection Phase is used to detect vascular degenerations from these images. In this study, the vein enlargement patterns in the images are detected by the object detection algorithm, too.

The system, which was prepared within the scope of the doctoral study (near-infrared images of the right and left forearms were used) and which enables the superficial veins (in the near-infrared images) to be visualized as an e-health application in the home environment, was re-trained in the study [1] to monitor the vein enlargement. In order to increase the low confidence values encountered in object detection in the study [1] and to perform a more sensitive detection, the system was re-trained with 4 different classes in this study. In addition, in the study [1], two artificial datasets (representing vein enlargements) created to be used in the training and testing processes of the You Only Look Once version-3 (YOLOv3) object detection algorithm were re-arranged. In this study, in addition to the processes described in the study [1], the Augmented Reality Phase, which is the 6th phase of the system, was also included in the study. In this way, it has been ensured that the detections and developments of vein enlargement can be visually presented to the user and his/her physician within the scope of Indirect Augmented Reality.

In Section II, both object detection studies within the scope of the YOLOv3 object detection algorithm and the virtual environment literature within the scope of Indirect Augmented Reality were examined. In Section III, Chronic Venous Disorder (CVD) types were introduced and the re-trained YOLOv3 object detection algorithm was explained so that the system can detect vein enlargement in the Object Detection Phase. How the datasets were created, which classes were defined and the results obtained as a result of the experiments were also stated in this section. In Section IV, how video-based images are arranged for the Augmented Reality Phase is detailed. In the last section, the study is discussed in general terms.

II. RELATED WORK

Classification processes are used to determine the class to which an image belongs. Traditional Convolutional Neural Networks can detect the belongingness of the inputs in the form of images, audio or video to defined classes. However, these networks do not give the position information of the objects they detect in the image. For this, object detection algorithms (Single Shot Detector SSD [18], Fast/Faster Region-based Convolutional Neural Networks [19]-[21], You Only Look Once YOLO [22]) are used. The YOLO algorithm is frequently preferred in studies especially because it can perform real-time object detection faster. In this context, YOLO version-3 [23] is included in this study because it can detect small objects as well [24].

In the study [25], which provides recognition of human movements and classification with location detection, the YOLO algorithm was trained using a total of 10 classes, including actions such as conversation between two people, exiting/entering the room, and handshaking. Images were processed as video streams and action recognition was performed with a small number of images (even a single image was sufficient in some cases).

In the study [26], which aims to provide real-time social distance detection in public areas within the scope of the Covid-19 pandemic, close proximity of more than 2 meters was detected by using the YOLOv3 object detection algorithm and marked with a red bounding box.

In the study [27], which performed fire detection as a real-time video-based tracking application, the tiny-YOLOv3 algorithm [28], a lighter version of the YOLOv3 object detection algorithm, was used. Experimental results obtained using 5000 training images and 5000 test images in the study confirmed the effectiveness of the proposed system.

In the study [29] investigating water consumption monitoring, the consumption indicator on the water meter counter images were determined by using the YOLOv4 algorithm [30], and the image was processed through the image processing stage and digit recognition was performed by converting it to black and white format. In addition, within the scope of the system developed in the study, a mobile application was made available. The study had an object detection accuracy of 98%.

In the study [31], which aimed to detect suspicious breast lesions on digital mammography images, early diagnosis and classification was performed using the YOLO algorithm. In

the study, 4 different classes were used as mass, calcification, architectural distortion and normal.

In the study [32], in which the YOLO algorithm was used for the detection of Diabetic retinopathy, which manifests with fundus lesions at its early level, fundus lesions were defined in 4 different classes as microaneurysms, hemorrhages, hard exudates and soft exudates.

In the study [33], which aims to detect Pediatric Pneumonia, Convolutional Neural Networks, which use X-Ray images as input, were used and it was aimed to accelerate the diagnosis decision process in this way. It was stated that the classification accuracy of the study for 3 different classes as normal, viral pneumonia, and bacterial pneumonia was 90.71%.

In the study [34], which aims to detect chest abnormality with deep learning, it had been underlined that doctors could be provided with a faster decision-making opportunity in diagnosing. In the study, Computed Tomography scan image inputs, a dataset of 18000 images (15000 train / 3000 test) labelled by radiologists, 14 different classes (Atelectasis, Calcification, Cardiomegaly, Consolidation, ILD, Infiltration, Lung Opacity, Nodule/Mass, Other lesions, Pleural effusion, Pleural thickening, Pneumothorax, Pulmonary fibrosis, No finding observation) and the YOLOv5 algorithm [35] were used.

In the system used in this study, Indirect Augmented Reality was used to present the CVD detection results obtained with the YOLOv3 object detection algorithm and their position in the image to the user/physician. Indirect Augmented Reality is a video-based virtual technology that has two separate modes, offline (creation of video visuals where virtual material is superimposed on real material) and online (displaying the superimposed video to the user in its real-world location). Studies in the literature on the concept are very limited.

In the study [36], which introduced the concept of Indirect Augmented Reality to the literature, previously recorded panoramic video images were used in two separate case studies within the scope of location finding and it was emphasized that the concept was useful for outdoor use.

In the study [37], in which it was stated that the alignment problems between virtual and real material could be solved with Indirect Augmented Reality, the participants gave positive feedback according to the results of the trials of virtual applications introducing Rome.

In the study [38], which combines both traditional Augmented Reality and Indirect Augmented Reality within the scope of the Casa Batlló museum promotion application in Spain, it was underlined that Indirect Augmented Reality could also be used as an indoor application. The application was also covered under the mobile-based Augmented Reality title. The application automatically switches between traditional and Indirect Augmented Reality according to the user's location. According to the results obtained in the study, the application can easily reflect the life of the beginning of the 20th century to the user.

In the study [39], that aims to eliminate temporal discrepancies (e.g., if online registration is performed at night while offline images are created with daytime images),

which are the negative aspects of Indirect Augmented Reality applications especially in outdoor use, samples taken from different environmental conditions at different times were added to the dataset. For online registration, a selection was made among the images in the dataset according to the histogram similarity.

In the study [40], which presents the Omaha Beach landing in an Indirect Augmented Reality environment, an environment was prepared in such a way that panoramic video images containing war scenes and narrations would be activated when the user was within 200 meters of the relevant region.

III. VEIN ENLARGEMENT DETECTION: DEEP LEARNING AND THE YOLOV3 OBJECT DETECTION ALGORITHM

Near-infrared imaging system is basically examined in two parts as hardware and software. While the hardware part is about the wavelength of the light source, Light Emitting Diode (LED) placements and camera features, the software part covers the extraction of vein patterns by making the veins in the obtained near-infrared images more prominent via digital image processing techniques. In this way, superficial veins can be visualized. The hardware part and digital image processing steps of the doctoral study were introduced in [3]. Also, the presentation of narrowing detections in processed images (using the YOLOv3 object detection algorithm with a single-class as *stenosis_vein*) to patient and his/her physician as a video-based Indirect Augmented Reality environment was explained in [4]. The 2-class vein enlargement patterns (*spider_vein* and *varicose_vein*) in the superficial vein images discussed in the study [1] were detailed as a total of 4 classes, with each 2 class represented by 2 levels (beginner and advanced) in this study.

When the superficial vein valves do not work properly, blood accumulations occur, and as a result, the veins expand, elongate, and form twisted folds, resulting in varicose veins [41][42]. Although varicose veins are most commonly observed in leg veins (which are under more pressure than other veins [41]), varicose veins can be encountered in any part of the body [43]. In general, however, the development of venous disorder in hand veins does not give results as dramatic as in leg veins. Chronic Venous Disorders (CVDs) affecting millions of people worldwide are caused by morphological and functional abnormalities of the venous system [44][45]. Risk factors such as heredity (family history, height), lifestyle (long term standing/sitting, occupation, smoking), gain (age, pregnancy, obesity, deep vein thrombosis) or hormones (female gender, progesterone) can lead to venous disorders, such as vein enlargement [46][47]. CVD clinical types are defined by the CEAP (Clinical, Etiological, Anatomical and Pathophysiological [44]) classification system (letter C represents "Class"): C0 (no visible signs of venous disease), C1 (visible veins, spider/telangiectasias veins), C2 (varicose veins), C3 (swelling/edema), C4 (changes to skin quality), C5 (healed ulceration), and C6 (active ulceration) [45][48]. CVD is often overlooked at its early levels [44]. In case of early diagnosis, advanced symptoms such as edema, skin changes

or leg ulcers can be alleviated with the support of lifestyle changes [45][47]. It was determined that the incidence of venous disorders in adults in urban and rural areas of Bonn in Germany was 59% for telangiectasias vein and 14% for varicose vein, respectively [45].

As most superficial veins, varicose veins are also not easily visible to the naked eye, so near-infrared light is used to visualize these veins [49]. In this study, the hand vein dataset (an example image from the dataset and its processed version are given in Fig. 1) obtained in the study [1] by using the superficial vein monitoring system was used for the experiments of the YOLOv3 object detection algorithm, which was re-trained to detect the beginner and advanced levels of CVD in the C1 (spider/telangiectasias veins) and C2 (varicose veins) types.

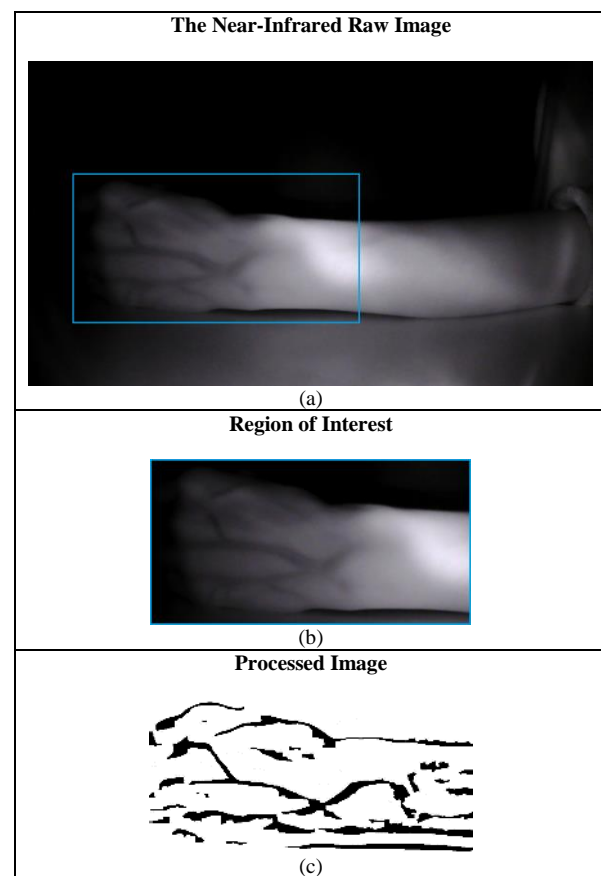


Figure 1. The near-infrared vein image. (a) The near-infrared raw image of hand dorsum. (b) Region of interest, containing only the veins to be examined. (c) Vein patterns obtained by digital image processing. [1]

The ability of the computer to make a determination (i.e., classification) on similar new data by using previously learned data is a decision-making process. Decision making is unique to biological creatures. However, nowadays computers can also "imitate" this process in various ways. This imitation is provided by Artificial Intelligence (the ability to imitate human-specific abilities such as recognition, classification, problem solving and learning by machines using various inputs such as image, sound and

signal [50]). In Machine Learning, which is a sub-branch of Artificial Intelligence, rule sets defined with expert knowledge (human factor) are needed to provide learning or to determine the distinctive features of the patterns [51]. In this way, various classification, regression or clustering operations (disease classification [52], stock forecasting [53] or airport passenger forecasting [54]) can be performed [51]. In Deep Learning, a sub-branch of Machine Learning, with the help of Artificial Neural Networks, features that cannot be detected by humans can be detected without any human intervention. In this way, learning is carried out via Deep Learning Algorithms by itself when only training and test data are given to the system as input. With Deep Learning, operations such as object recognition, speech recognition or object detection can be provided [55].

The YOLOv3 is a Deep Learning Algorithm that performs object detection. With Object Detection Algorithms, training can be performed for multiple objects (up to 80 classes [23] placed at certain positions on the image) that can represent different classes. The YOLOv3 object detection algorithm marks the positions of the objects detected onto the image with bounding boxes. In addition, the name and detection rate (confidence value is shown between 0.00 and 1.00 in the study) of the class with the highest probability to which the object may belong are printed on the box.

In this study, the YOLOv3 object detection algorithm was used for CVD detection in vein patterns obtained by image processing steps. The developed near-infrared imaging system was re-trained in this study to detect 2 different CVD types (C1 and C2) as 4 classes (spider_beginner, spider_advanced, varicose_beginner and varicose_advanced).

There is currently no venous disorder dataset consisting of near-infrared images, available to the public. For this, in this study, a new 4-class (to detect vascular degenerations in more detail) training dataset was prepared by adding artificial patterns on to near-infrared images (the dataset, which is also used in the study [1], was created by the method of obtaining images from video recordings described in the study [4]). The new dataset used in this study was prepared with images that each contain 10 spider_beginner and 10 spider_advanced artificial patterns, and each 5 varicose_beginner and 5 varicose_advanced artificial patterns (the dataset in the study [1] contains 150 near-infrared images, each containing 5 spider_vein and 5 varicose_vein patterns). Furthermore, 50 additional images were created (as in the study [1]) from the existing images by data augmentation methods (10-degree rotation, 30-degree rotation, mirroring, noise addition and downscaling). In this way, a (4-class) training dataset with 6000 artificial patterns was obtained (in the study [1], a (2-class) dataset with 2000 artifacts including 1000 spider_vein and 1000 varicose_vein patterns was used). The patterns in the images were labelled with the free (under General Public License version 3) makesense [56] web-based application.

A second dataset consisting of 600 images containing artificial vein enlargement patterns was prepared for the test

process to be carried out after the trainings (in the study [1] the test dataset consists of 300 images). The test dataset was created by adding only a single pattern (artificial patterns not used in the training) to each image in random rotations and positions (preserving a certain figural format, 150 patterns for each class) (the dataset used in [1] was created by adding only one spider_vein or varicose_vein pattern). In this way, a test dataset of 600 images with 4 classes containing 150 patterns was obtained (in the study [1], a test dataset of 300 images in total was obtained, with 150 test images containing spider_vein class and 150 test images containing varicose_vein class). The confusion matrix of the object detection results of the YOLOv3 object detection algorithm, obtained by using the test dataset is given in Table I for the study [1] (for comparison purposes) and in Table II for this study. As can be seen from the matrix, all of the searched objects (spider_beginner, spider_advanced, varicose_beginner and varicose_advanced patterns) in the test images were detected correctly (for the study [1], all of the spider_vein and varicose_vein patterns were detected correctly). The developed system can detect CVD patterns in C1 and C2 types with Accuracy Rate (1), Misclassification Rate (0), Precision (1), Prevalence (0.5) and F-Score (1) values (similar to the study [1]). 10 sample patterns for each class with the YOLOv3 object detection algorithm confidence values marked are given in Table III.

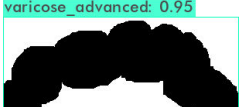
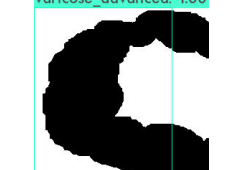
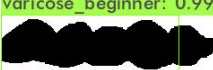
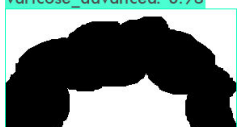
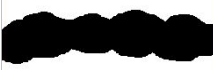
TABLE I. THE CONFUSION MATRIX OF THE YOLOV3 OBJECT DETECTION ALGORITHM RESULTS OBTAINED WITH SPIDER_VEIN AND VARICOSE_VEIN CLASSES [1]

		Predicted Class	
		spider_vein (Positive)	varicose_vein (Negative)
Actual Class	spider_vein (Positive)	True Positive=150	False Negative=0
	varicose_vein (Negative)	False Positive=0	True Negative=150

TABLE II. THE CONFUSION MATRIX OF THE YOLOV3 OBJECT DETECTION ALGORITHM RESULTS OBTAINED WITH SPIDER_BEGINNER, SPIDER_ADVANCED, VARICOSE_BEGINNER AND VARICOSE_ADVANCED CLASSES

		Predicted Class				
		spider beginner	spider advanced	varicose beginner	varicose advanced	unclassified
Actual Class	spider beginner	150	0	0	0	0
	spider advanced	0	150	0	0	0
	varicose beginner	0	0	150	0	0
	varicose advanced	0	0	0	150	0

TABLE III. CONFIDENCE VALUE RESULTS OF THE YOLOV3 OBJECT DETECTION ALGORITHM FOR SPIDER_BEGINNER, SPIDER_ADVANCED, VARICOSE_BEGINNER AND VARICOSE_ADVANCED CLASS PATTERNS

#	spider_beginner	spider_advanced	varicose_beginner	varicose_advanced
1	spider_beginner: 0.86 	spider_advanced: 0.88 	varicose_beginner: 0.99 	varicose_advanced: 0.99 
2	spider_beginner: 0.94 	spider_advanced: 0.91 	varicose_beginner: 0.98 	varicose_advanced: 0.95 
3	spider_beginner: 0.55 	spider_advanced: 0.92 	varicose_beginner: 0.99 	varicose_advanced: 1.00 
4	spider_beginner: 0.85 	spider_advanced: 0.80 	varicose_beginner: 0.82 	varicose_advanced: 1.00 
5	spider_beginner: 0.97 	spider_advanced: 0.90 	varicose_beginner: 0.99 	varicose_advanced: 0.98 
6	spider_beginner: 0.75 	spider_advanced: 0.91 	varicose_beginner: 0.91 	varicose_advanced: 0.98 
7	spider_beginner: 1.00 	spider_advanced: 0.98 	varicose_beginner: 0.91 	varicose_advanced: 0.99 
8	spider_beginner: 0.95 	spider_advanced: 0.98 	varicose_beginner: 0.95 	varicose_advanced: 1.00 
9	spider_beginner: 0.87 	spider_advanced: 0.83 	varicose_beginner: 0.93 	varicose_advanced: 1.00 
10	spider_beginner: 0.83 	spider_advanced: 0.98 	varicose_beginner: 0.98 	varicose_advanced: 1.00 

The venous disorder detection confidence values of the YOLOv3 object detection algorithm performed with sample images of the C1 type of CVD are shown in Fig. 2 (a, b, c) for spider_vein (0.99) [1], spider_beginner (0.99) and spider_advanced (1.00). Also, confidence values for C2 type are shown in Fig. 3 (a, b, c) for varicose_vein (0.90) [1], varicose_beginner (0.98) and varicose_advanced (0.98). Although all classes in the test images were predicted correctly in the study [1], the YOLOv3 object detection algorithm had a lower confidence value for some patterns. As stated in Table IV, in the study [1], among 150 images

containing spider_vein patterns, 130 had a confidence value in the range of 0.95-1.00, 13 in the range of 0.90-0.94, 6 in the range of 0.80-0.89, and 1 of them was determined as 0.32. When the pattern with the confidence value of 0.32 is examined, it is determined that it is not much different from the patterns in the training dataset (mostly large-sized patterns were used) or other test patterns, but it is smaller in size, as can be seen in Fig. 4 (a). It was evaluated that this situation may result in a low confidence value.

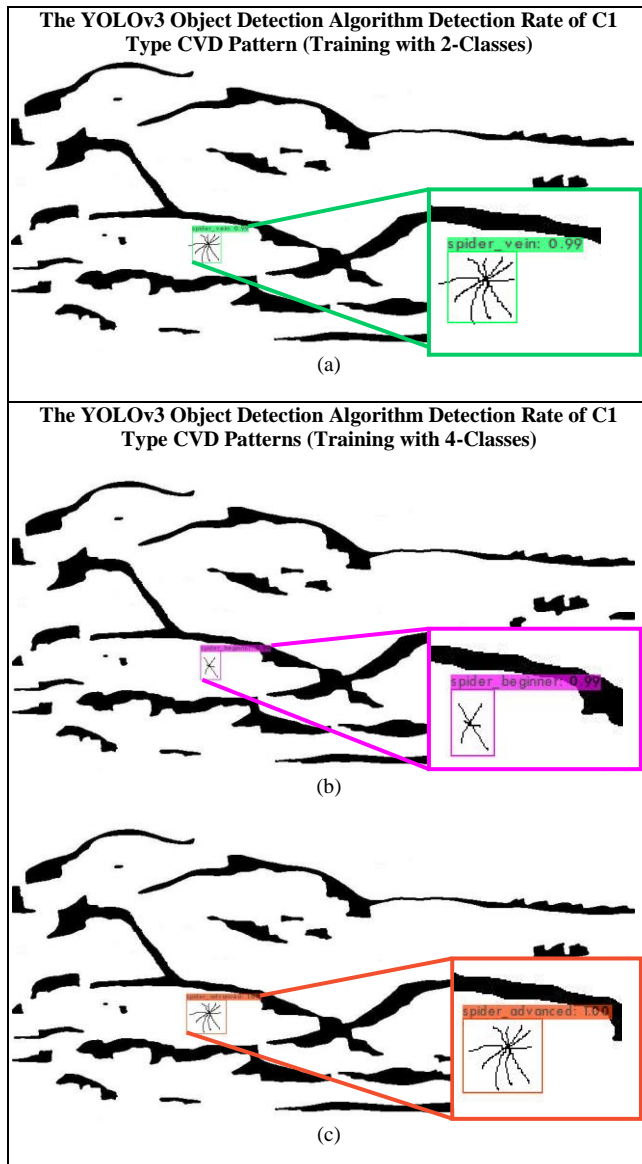


Figure 2. The YOLOv3 object detection algorithm test process result image samples for C1 type CVD patterns. (a) 0.99 confidence valued result for spider_vein class [1]. (b) 0.99 confidence valued result for spider_beginner class. (c) 1.00 confidence valued result for spider_advanced class.

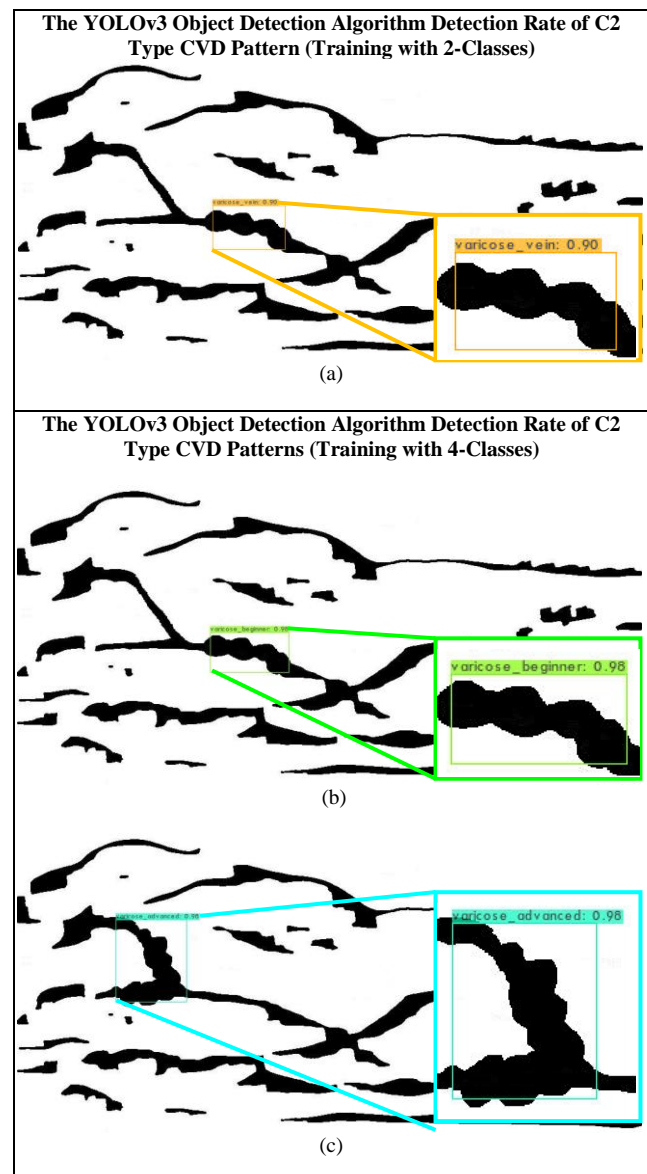


Figure 3. The YOLOv3 object detection algorithm test process result image samples for C2 type CVD patterns. (a) 0.90 confidence valued result for varicose_vein class [1]. (b) 0.98 confidence valued result for varicose_beginner class. (c) 0.98 confidence valued result for varicose_advanced class.

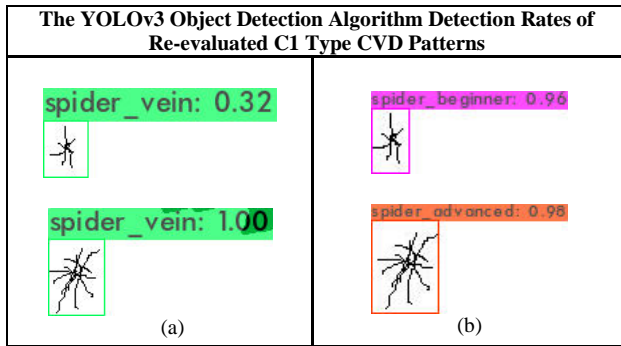


Figure 4. C1 type CVD patterns shown in accordance with their actual dimensions. (a) Patterns with confidence values of 0.32 and 1.00 belonging to the spider_vein class [1]. (b) Patterns with confidence values of 0.96 and 0.98 belonging to the spider_beginner and spider_advanced classes, respectively.

In this study, for control purposes, the CVD artificial patterns that were detected with low confidence values in the study [1] were re-examined. For this reason, spider_beginner patterns (smaller sized and less branched spider_vein patterns to represent the beginner level of C1) were added to the dataset in this study. Spider_vein detection with a confidence value of 0.32 obtained in [1] was determined as a spider_beginner with a confidence value of 0.96 according to the results of the YOLOv3 object detection algorithm trained with 4 classes, as in Fig. 4 (b). This shows that the system can also detect vascular degenerations in smaller sizes (at the beginner level).

As shown in Table IV, again in the study [1], among the 150 images containing varicose_vein pattern, 126 had a confidence value in the range of 0.95-1.00, 6 had a range of 0.90-0.94, 11 had a range of 0.80-0.89, and 7 had a range of 0.79-0.30. When the 7 patterns with the lowest confidence values are examined, it is determined that these patterns are slightly different (U-shaped, twisted) from the patterns in the training dataset or other test patterns (mostly linear line patterns were used) which can be seen in Fig. 5 (a). It was evaluated that this condition may lead to a low confidence value. Therefore, in this study, varicose_advanced patterns (U-shaped and twisted patterns of varicose_veins to represent the advanced level of C2) were added to the dataset. According to the results of the YOLOv3 object detection algorithm trained with 4 classes, the varicose_vein pattern with a confidence value of 0.30 obtained in the study [1] was determined as the varicose_advanced pattern with a confidence value of 0.94 as in Fig. 5 (b). This indicates that the system can also detect vascular degenerations when the patterns become more twisted (for monitoring progress at advanced levels).

Since small-sized spider_vein patterns represent the early levels of CVD (spider_beginner) and varicose_vein patterns can also twist and fold (may not follow a linear line) over time (varicose_advanced), such patterns are important in the scope of detection system. Therefore, in order to overcome the low confidence values of spider_vein and varicose_vein classes described in the study [1], new smaller-sized patterns and also new U-shaped patterns were added to the training dataset with different rotations.

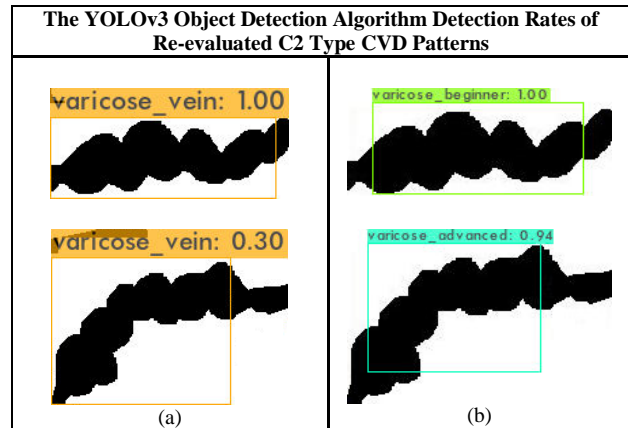


Figure 5. C2 type CVD patterns shown in accordance with their actual dimensions. (a) Patterns with confidence values of 1.00 and 0.30 belonging to the varicose_vein class [1]. (b) Patterns with confidence values of 1.00 and 0.94 belonging to the varicose_beginner and varicose_advanced classes, respectively.

Examining Table V showing the results obtained, it can be seen that out of 150 images containing spider_beginner pattern, 68 of them had confidence values in the range of 0.95-1.00, 28 of them in the range of 0.90-0.94, 43 of them in the range of 0.80-0.89, and 11 of them in the range of 0.79-0.55. For the spider_advanced pattern, the confidence values for 113 images were found to be in the range of 0.95-1.00, 16 of them between 0.90-0.94, 12 of them between 0.80-0.89, and 9 of them between 0.79-0.63. Looking at Table V for the varicose_beginner pattern, 135 confidence values were found between 0.95-1.00, 10 between 0.90-0.94, 3 between 0.80-0.89, and 2 confidence values between 0.79-0.63. For the varicose_advanced pattern, 145 confidence values were found between 0.95-1.00, 3 between 0.90-0.94, 1 between 0.80-0.89, and 1 between 0.79-0.63. The number of CVD types' confidence results obtained in this study, especially in the range of 0.95-1.00, is greater for the C2 (varicose_vein) type (280 confidence values) than for the C1 (spider_vein) type (181 confidence values). This shows that the system can detect varicose levels with higher confidence. In addition, as it can be seen from Table II, the fact that no misclassification has been made in the system proves that the system works extremely effectively in the detection of both CVD types and progress.

The confidence value arithmetic mean (0.973) of the single-class C1 type (spider_vein) in Table IV is slightly higher than the arithmetic mean (0.912 and 0.953) of the two-class C1 type (spider_beginner and spider_advanced) in Table V. Since, the patterns of spider_vein and varicose_vein are very different from each other in shape, it provides an easier distinction (130 spider_vein patterns were correctly classified with a confidence value in the range of 0.95-1.00, which increased the arithmetic mean). This less significant decrease in the test results of the system in this study is a result of the distribution of the confidence values to different detection intervals (0.95-1.00, 0.90-0.94, 0.80-0.89 and 0.79-0.00) when the C1 type is divided into two separate classes with basically similar pattern formats. On the other hand, the fact that the minimum confidence values (0.55 and 0.63) in

Table V for C1 type are higher than those in Table IV (0.32), it draws attention to the fact that a more precise classification decision can be made.

TABLE IV. RESULTS OF CONFIDENCE VALUES FOR THE YOLOV3 OBJECT DETECTION ALGORITHM TRAINED WITH TWO CLASSES [1]

n=300 (150 for each class)	C1: spider vein	C2: varicose vein
Arithmetic Mean	0.973	0.955
Minimum	0.32	0.30
Maximum	1.00	1.00
[0.95-1.00] Range	130	126
[0.90-0.94] Range	13	6
[0.80-0.89] Range	6	11
[0.79-0.00] Range	1	7

TABLE V. RESULTS OF CONFIDENCE VALUES FOR THE YOLOV3 OBJECT DETECTION ALGORITHM TRAINED WITH FOUR CLASSES

n=600 (150 for each class)	C1: spider beginner	C1: spider advanced	C2: varicose beginner	C2: varicose advanced
Arithmetic Mean	0.912	0.953	0.982	0.993
Minimum	0.55	0.63	0.67	0.79
Maximum	1.00	1.00	1.00	1.00
[0.95-1.00] Range	68	113	135	145
[0.90-0.94] Range	28	16	10	3
[0.80-0.89] Range	43	12	3	1
[0.79-0.00] Range	11	9	2	1

Looking at Table IV and Table V for C2 type CVD (varicose_vein), it can be seen that the two-class arithmetic mean results (0.982 and 0.993) are higher than the one-class result (0.955). It was evaluated that the introduction of U-shaped patterns to the system (due to the use of flat shaped patterns for training, twists are detected with lower confidence values in Table IV) contributed to this situation. In addition, as can be seen from Table V, the confidence value determinations for both levels of the C2 type are especially concentrated in the range of 0.95-1.00. In addition, the minimum confidence values (0.67 and 0.79) in Table V for C2 type were higher than those in Table IV (0.30). These cases also reinforce that the system can make a classification decision with higher precision.

IV. INDIRECT AUGMENTED REALITY

Virtual technologies are used in every imaginable field, especially health, education, construction, agriculture, tourism and entertainment. Although these technologies are known as virtual reality with the most popular definition among the public, they are called virtual environments in academic context [57]. The goal of virtual environments is to create a perception of reality in the user. The degree of perception of reality can be determined by criteria such as sense of presence, immersion, real-time and interaction [58]-[61]. While the user's mental feeling in the virtual environment expresses the "sense of presence" criterion, the coverage of the user's field of view with the physical hardware expresses the "immersion" criterion, and the manipulation of the environment in "real-time" expresses the

"interaction" criterion. The more these criteria can be supported, the more the environment is perceived as real by the user. The perception of reality is application-specific. For example, while the main goal in computer games is to create a feeling of reality, in some educational applications, only the visualization of 3-D concepts can be aimed. The type of virtual environment to be designed according to the target and the devices to be used are determined. Milgram's Reality-Virtuality Continuum [62] is one of the most basic classifications used for virtual environments. In this Continuum, there are Virtual Environment (containing completely virtual material) and Real Environment (containing completely real material) under the main heading of Mixed (Hybrid) Reality. In the case of a mixture of these two environments, the concepts of Augmented Virtuality (contains virtual material more than real ones) and Augmented Reality (contains real material more than virtual ones) are defined.

The aim of this study is to present the confidence values and positions (virtual material) of CVD development to the user and his/her physician as a low-cost early diagnosis system within the scope of e-health service. For this reason, the method of providing access to these contents from mobile device screens has been preferred instead of high-cost devices. Although, monitoring the virtual content from a small screen minimizes the perception of reality (due to lack of immersion), it is considered useful within the scope of the study. However, the computing capacity and hardware features of a mobile device are insufficient for the operations to be performed in the 6-phase system used. For this, all operations in the system (except the Imaging Technique Phase) are carried out on the server and processed video visuals (containing only virtual-real material with calculation results) are returned to the user/physician.

Although one of the important criteria in Augmented Reality applications is real-time, there is a visualization spread over a long time interval (to support monitoring at certain periods) in this study. For this reason, real-time of visuals is supported only when the region where the relevant tissue is displayed and the class of the images stored on the server match (requires Classification Phase to be used for a second test). Displaying videos of the matched class on the screen in this way is examined under Indirect Augmented Reality [36]. Indirect augmented reality is especially suited for outdoor use [36]. Its basis is the superimposition (overlay of virtual and real material) of virtual models of structures/places in their real locations while displaying them in their real environment. Two separate registration (spatial alignment of virtual and real material) methods (offline and online registration) are used in Indirect Augmented Reality [39]. Offline registration is combining the pre-recorded video of the relevant tissue with the virtual model. In the offline registration in this study, the YOLOv3 object detection algorithm confidence values and positions of the CVD detected in the digitally processed image are superimposed on the near-infrared raw video recordings. Online registration, on the other hand, is the real-time superimposition of the superimposed video prepared in offline registration on the relevant tissue viewed in the real

world. In the online registration of this study, offline video visuals are presented to the user in real-time when the tissue region to which they belong is displayed.

Among the advantages of using Indirect Augmented Reality within the scope of this study, having low-cost and low computational/processing load requirements (effective for use on mobile devices as no additional hardware is required), tight matching of virtual and real material with offline registration (effective for displaying the vein position on the relevant tissue), and offering a time-independent visualization as before/after (effective for tracking CVD development process from images obtained at certain periods) can be counted [36][40][63].

In the offline registration of this study, on near-infrared raw image(s) (it is the real material captured in the Imaging Technique Phase and shown in Fig. 6 (a)), processed image(s) (it is virtual material processed by the Digital Image Post-Processing Phase and shown in Fig. 6 (b)) and their YOLOv3 object detection algorithm results (it is the virtual material obtained from the Object Detection Phase and shown in Fig. 6 (c)) were superimposed, as depicted in Fig. 6 (d) and video visuals of the relevant period were created. As online registration, these superimposed video visuals are presented to the user/physician via the mobile device (smartphone) screen when the relevant tissue is displayed, as shown in Fig. 6 (e).

V. CONCLUSION AND FUTURE WORK

Visualization of superficial veins by using near-infrared light is among the applications currently used in the healthcare industry. This imaging technique, which is especially useful for vascular access and is harmless to the body, was used in this study within the scope of early diagnosis. The superficial vein monitoring system, which was prepared within the scope of the doctoral study, was re-trained in this study to detect Chronic Venous Disorder with 4 different classes (spider_beginner, spider_advanced, varicose_beginner and varicose_advanced). In this study, all of the artificial vein enlargement patterns in the test images could be accurately detected by using the You Only Look Once version-3 object detection algorithm and no misclassification was encountered. The absence of misclassification can show that the proposed system is particularly useful for the health sector. The classes and their detection rates of the tested patterns are marked on the resulting image as the class name and the confidence value. The developed system was able to detect the classes of objects with the values of Accuracy Rate (1), Misclassification Rate (0), Precision (1), Prevalence (0.5) and F-Score (1). In addition to the class detection, the pattern positions are also determined with the help of this algorithm and marked on the images. Also, a video-based indirect augmented reality environment was integrated into the study for the monitoring of 4 classes of superficial vein enlargement, thus informing the patient and the physician.

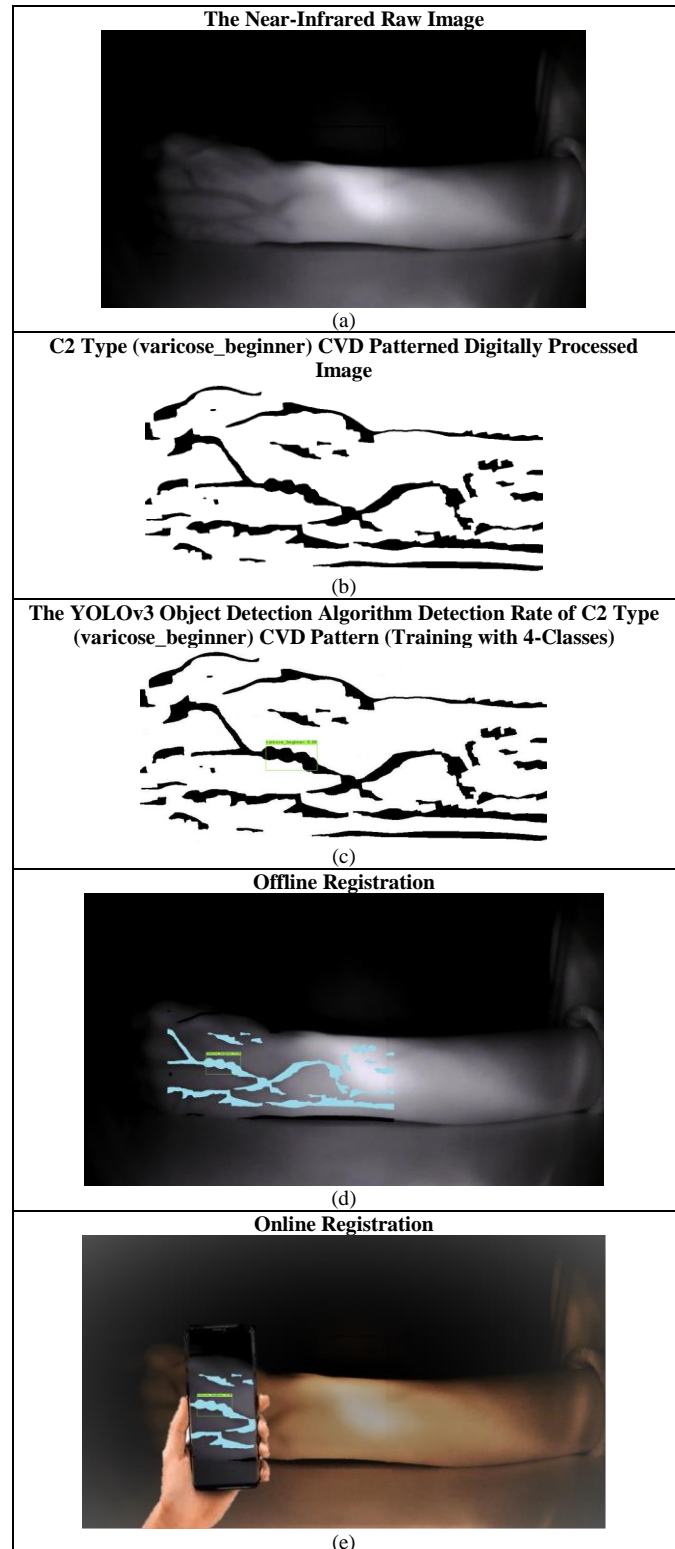


Figure 6. Indirect augmented reality offline registration and online registration for C2 type CVD pattern (varicose_beginner). (a) The near-infrared raw image. (b) Digitally processed image with artificial varicose_beginner pattern added. (c) The YOLOv3 object detection algorithm confidence value obtained with the 4-class training. (d) Offline registration. (e) Online registration.

On the other hand, black pixels that may occur on the image due to the illumination or imaging can have a negative effect on the detection process. In the experiments, this situation was encountered in a few images. It was observed that the dense accumulation of these pixels in a certain region makes detections of the spider_beginner type (due to its small size), which does not actually exist, albeit with low confidence values (0.25, 0.30). However, when considered within the scope of video visuals, these determinations in one or more images were not taken into account, since there are 100 or more image combinations.

Detection of Class-1 type (spider/telangiectasias vein) of Chronic Venous Disorder is of very critical importance especially in determining the transition process to Class-2 type (varicose vein) and the treatment process. In this respect, the most important benefit of the indirect augmented reality environment within the scope of this system and early diagnosis is that it allows visualization in the form of before and after presentation. In this way, treatment can be started and directed without delay. Although the system has been tested with near-infrared data and artificial patterns, it is planned to test the system on real patients within the scope of future studies. In addition, it is considered that the proposed system can shed light on researchers who want to make similar determinations on images obtained with different imaging techniques.

REFERENCES

- [1] H. A. Erdem and S. Utku, "Detecting Venous Disorders via Near-infrared Imaging: Observation of Varicose Vein Development", The IARIA Annual Congress on Frontiers in Science, Technology, Services, and Applications (IARIA Congress 2022), IARIA, Jul. 2022, pp. 65-68, Nice, France. https://www.thinkmind.org/index.php?view=article&articleid=iaria_congress_2022_1_130_50088
- [2] H. A. Erdem, "Integrating Detection of Vascular Degeneration into Augmented Reality Environment: An E-Health Application Based on Near-Infrared Spectroscopy and Deep Learning", Doctoral Dissertation, Dokuz Eylül University, İzmir, Turkey, Aug. 2022. https://tez.yok.gov.tr/UlusalTezMerkezi/TezGoster?key=kIrlFdtdJ31bRgjb6fHvMUaznxXZ9naUDrsv_v_8KDNe7rlBiHk9Ti8ryVaaMRGz
- [3] H. A. Erdem, I. Erdem, and S. Utku, "Near-Infrared Mobile Imaging Systems for E-Health: Lighting the Veins". The Twelfth International Conference on eHealth, Telemedicine, and Social Medicine (eTELEMED), Nov. 2020, IARIA, pp. 80-84, Valencia, Spain. https://www.thinkmind.org/index.php?view=article&articleid=etelemed_2020_3_90_40039
- [4] H. A. Erdem and S. Utku, "Augmented Reality Aided Pre-Diagnosis Environment for Telemedicine: Superficial Vein Surveillance System". European Journal of Science and Technology, vol. 38, pp. 376-385, Aug. 2022. <https://doi.org/10.31590/ejosat.1107531>
- [5] M. Y. M. Chen, T. L. Pope, and D. J. Ott, Basic Radiology, 2nd ed., McGraw Hill: Lange Clinical Medicine, 2011.
- [6] Inside View: A Blog For Our Patients, From UVA Radiology and Medical Imaging. *Different Imaging Tests, Explained*. 17.Sep.2017. [Online]. Available from: <https://blog.radiology.virginia.edu/different-imaging-tests-explained/> [retrieved: May, 2023]
- [7] Bravo Imaging. *Medical Imaging Modality Options and Their Uses*. 20.Jul.2008. [Online]. Available from: <https://www.bravoimaging.com/medical-imaging-equipment-miami/medical-imaging-modality-options-and-their-uses/> [retrieved: May, 2023]
- [8] V. P. Zharov et al., "Infrared Imaging of Subcutaneous Veins", *Lasers in Surgery and Medicine: The Official Journal of the American Society for Laser Medicine and Surgery*, 34(1), pp. 56-61, 2004. <https://doi.org/10.1002/lsm.10248>
- [9] R. Fuksis, M. Greitans, O. Nikisins, and M. Pudzs, "Infrared Imaging System for Analysis of Blood Vessel Structure", *Electronics and Electrical Engineering, System Engineering, Computer Technology*, 97(1), pp. 45-48, 2010. <https://eejournal.ktu.lt/index.php/elt/article/view/9943>
- [10] N. Bouzida, A. H. Bendada, and X. P. Maldague, "Near-Infrared Image Formation and Processing for the Extraction of Hand Veins", *Journal of Modern Optics*, 57(18), pp. 1731-1737, 2010. <https://doi.org/10.1080/09500341003725763>
- [11] Enclopedia Britannica, *Hemoglobin*. [Online]. Available from: <https://www.britannica.com/science/hemoglobin> [retrieved: May, 2023]
- [12] S. Crisan, "A novel perspective on hand vein patterns for biometric recognition: Problems, challenges, and implementations", in *Biometric security and privacy. Signal Processing for Security Technologies*, R. Jiang, S. Al-Maadeed, A. Bouridane, P. Crookes, and A. Beghdadi, Eds. Springer International Publishing, Cham., pp. 21-49, 2017. https://doi.org/10.1007/978-3-319-47301-7_2
- [13] Y. Ayoub et al., "Diagnostic Superficial Vein Scanner", International Conference on Computer and Applications (ICCA 2018), Aug. 2018, IEEE, pp. 321-325. <https://doi.org/10.1109/COMAPP.2018.8460229>
- [14] Royal Society of Chemistry, *Introduction to Spectroscopy*. [Online]. Available from: <https://edu.rsc.org/download?ac=11384> [retrieved: May, 2023]
- [15] H. Bay, T. Tuytelaars, and L. Van Gool, "SURF: Speeded up robust features", in *Computer vision-European Conference on Computer Vision Lecture Notes in Computer Science*, vol 3951. A. Leonardis, H. Bischof, and A. Pinz, Eds. Springer, Berlin, Heidelberg, pp. 404-417, 2006. https://doi.org/10.1007/11744023_32
- [16] C. L. Lin and K. C. Fan, "Biometric Verification Using Thermal Images of Palm-Dorsa Vein Patterns", *IEEE Transactions on Circuits and Systems for Video Technology*, 14(2), pp. 199-213, 2004. <https://doi.org/10.1109/TCSVT.2003.821975>
- [17] R. Garcia-Martin and R. Sanchez-Reillo, "Vein Biometric Recognition on a Smartphone", *IEEE Access*, 8, pp. 104801-104813, 2020. <https://doi.org/10.1109/ACCESS.2020.3000044>
- [18] W. Liu et al., "SSD: Single Shot Multibox Detector", *Computer Vision-ECCV 14th European Conference, Amsterdam, The Netherlands, Part I 14 Springer International Publishing*, October 2016, pp. 21-37. <https://arxiv.org/abs/1512.02325>
- [19] R. Girshick, J. Donahue, T. Darrell, and J. Malik, "Rich Feature Hierarchies for Accurate Object Detection and Semantic Segmentation", In: *Proceedings of the IEEE conference on computer vision and pattern recognition*, 2014, IEEE, pp. 580-587. <https://arxiv.org/abs/1311.2524>
- [20] R. Girshick, "Fast R-CNN", In: *Proceedings of the IEEE International Conference on Computer Vision*, 2015, pp. 1440-1448. <https://arxiv.org/abs/1504.08083>
- [21] S. Ren, K. He, R. Girshick, and J. Sun, "Faster R-CNN: Towards Realtime Object Detection with Region Proposal Networks", *Advances in Neural Information Processing Systems (NIPS)*, 2015, pp. 91-99. <https://arxiv.org/abs/1506.01497>

- [22] J. Redmon, S. Divvala, R. Girshick, and A. Farhadi, "You Only Look Once: Unified, Real-Time Object Detection", In: Proceedings of the IEEE Conference on Computer Vision and Pattern Recognition (CVPR), 2016, pp. 779-788.
- [23] J. Redmon and A. Farhadi, "YOLOv3: An Incremental Improvement", Arxiv preprint, 2018. <https://doi.org/10.48550/arXiv.1804.02767>
- [24] H. Bandyopadhyay, *YOLO: Real-Time Object Detection Explained*. [Online]. Available from: <https://www.v7labs.com/blog/yolo-object-detection> [retrieved: May, 2023]
- [25] S. Shinde, A. Kothari, and V. Gupta, "YOLO Based Human Action Recognition and Localization", *Procedia Computer Science*, 2018, 133, pp. 831-838. <https://doi.org/10.1016/j.procs.2018.07.112>
- [26] K. S. Babulal et al., "Real-Time Surveillance System for Detection of Social Distancing", *International Journal of E-Health and Medical Communications (IJEHMC)*, vol. 13(4), pp. 1-13, 2022. <https://doi.org/10.4018/IJEHMC.309930>
- [27] L. W. Kang, I. S. Wang, K. L. Chou, S. Y. Chen, and C. Y. Chang, "Image-Based Real-Time Fire Detection Using Deep Learning with Data Augmentation for Vision-Based Surveillance Applications", *The 16th IEEE International Conference on Advanced Video and Signal Based Surveillance (AVSS 2019)*, IEEE, Sept. 2019, pp. 1-4. <https://doi.org/10.1109/AVSS.2019.8909899>
- [28] R. Huang, J. Pedoeem, and C. Chen, "YOLO-LITE: A Real-Time Object Detection Algorithm Optimized for Non-GPU Computers", In: 2018 IEEE International Conference on Big Data (Big Data). IEEE, 2018. pp. 2503-2510. <https://doi.org/10.48550/arXiv.1811.05588>
- [29] J. Ktari, T. Frikha, M. Hamdi, H. Elmannai, and H. Hmam, "Lightweight AI Framework for Industry 4.0 Case Study: Water Meter Recognition", *Big Data and Cognitive Computing*, 2022, vol. 6(3), 72, July 2022. <https://doi.org/10.3390/bdcc6030072>
- [30] A. Bochkovskiy, C. Y. Wang, and H. Y. M. Liao, "YOLOv4: Optimal Speed and Accuracy of Object Detection", ArXiv preprint, 2020. <https://doi.org/10.48550/arXiv.2004.10934>
- [31] A. Baccouche, B. Garcia-Zapirain, Y. Zheng, and A. S. Elmaghaby, "Early Detection and Classification of Abnormality in Prior Mammograms Using Image-to-Image Translation and YOLO Techniques", *Computer Methods and Programs in Biomedicine*, vol. 221, Jun. 2022. <https://doi.org/10.1016/j.cmpb.2022.106884>
- [32] C. Santos, M. Aguiar, D. Welfer, and B. Belloni, "A New Approach for Detecting Fundus Lesions Using Image Processing and Deep Neural Network Architecture Based on YOLO Model", *Sensors*, vol. 22 (17), Aug. 2022. <https://doi.org/10.3390/s22176441>
- [33] E. Ayan, B. Karabulut, and H. M. Ünver, "Diagnosis of Pediatric Pneumonia with Ensemble of Deep Convolutional Neural Networks in Chest X-Ray Images", *Arabian Journal for Science and Engineering*, vol. 47, pp. 2123-2139, Sept. 2022. <https://doi.org/10.1007/s13369-021-06127-z>
- [34] Y. Luo, Y. Zhang, X. Sun, H. Dai, and X. Chen, "Intelligent Solutions in Chest Abnormality Detection Based on YOLOv5 and ResNet50", *Journal of Healthcare Engineering*, vol. 2021, Oct. 2021. <https://doi.org/10.1155/2021/2267635>
- [35] R. Couturier, H. N. Noura, O. Salman, and A. Sider, "A Deep Learning Object Detection Method for an Efficient Clusters Initialization", Arxiv preprint, 2021. <https://doi.org/10.48550/arXiv.2104.13634>
- [36] J. Wither, Y. T. Tsai, and R. Azuma, "Indirect Augmented Reality", *Computers and Graphics*, vol. 35(4), pp. 810-822, Aug. 2011. <https://doi.org/10.1016/j.cag.2011.04.010>
- [37] G. Liestol and A. Morrison, "Views, Alignment and Incongruity In Indirect Augmented Reality", 2013 IEEE International Symposium on Mixed and Augmented Reality - Arts, Media, and Humanities (ISMAR-AMH), Adelaide, SA, Australia, pp. 23-28, 2013. <https://doi.org/10.1109/ISMAR-AMH.2013.6671263>
- [38] J. Gimeno, C. Portales, I. Coma, M. Fernandez, and B. Martinez, "Combining Traditional and Indirect Augmented Reality for Indoor Crowded Environments: A Case Study on the Casa Batllo Museum", *Computers and Graphics*, vol. 69, pp. 92-103, Dec. 2017. <https://doi.org/10.1016/j.cag.2017.09.001>
- [39] F. Okura, T. Akaguma, T. Sato, and N. Yokoya, "Indirect Augmented Reality Considering Real-World Illumination Change", In Proceedings of the IEEE International Symposium on Mixed and Augmented Reality (ISMAR), IEEE, Sept. 2014, pp. 287-288, Munich, Germany. <https://doi.org/10.1109/ISMAR.2014.6948453>
- [40] G. Liestoel, "Augmented Reality Storytelling: Narrative Design And Reconstruction Of A Historical Event In Situ", *International Journal of Interactive Mobile Technologies*, vol. 13(12), pp. 96-209, 2019. <https://doi.org/10.3991/ijim.v13i12.11560>
- [41] N. Özbayrak, "Varis Çoraplarının Performans Özelliklerinin İncelenmesi (An Investigation About Performance Properties of Compression Stockings)", Master's Thesis, Uludağ University, Bursa, Turkey, Jul. 2009. Thesis in Turkish with an abstract in English. <http://hdl.handle.net/11452/3321>
- [42] A. E. Gabbey and J. Marcin (reviewed by), Healthline. *Varicose Veins*. 8.Mar.2019. [Online]. Available from: <https://www.healthline.com/health/varicose-veins> [retrieved: May, 2023]
- [43] Health. Johns Hopkins Medicine. *Varicose Veins*. [Online]. Available from: <https://www.hopkinsmedicine.org/health/conditions-and-diseases/varicose-veins> [retrieved: May, 2023]
- [44] T. Feodor, S. Baila, I. A. Mitea, D. E. Branisteanu, and O. Vittos, "Epidemiology and Clinical Characteristics of Chronic Venous Disease in Romania", *Experimental and Therapeutic Medicine*, vol. 17(2), pp. 1097-1105, Dec. 2019. <https://doi.org/10.3892/etm.2018.7059>
- [45] H. Partsch, "Varicose Veins and Chronic Venous Insufficiency", *Vasa: European Journal of Vascular Medicine*, 38(4), pp. 293-301, Jan. 2009. <https://doi.org/10.1024/0301-1526.38.4.293>
- [46] G. Piazza, "Varicose Veins", *Circulation*, vol. 130(7), pp. 582-587, Aug. 2014. <https://doi.org/10.1161/CIRCULATIONAHA.113.008331>
- [47] N. Labropoulos, "How Does Chronic Venous Disease Progress from the First Symptoms to the Advanced Stages? A Review". *Advances in Therapy*, vol. 36(1), pp. 13-19, Feb. 2019. <https://doi.org/10.1007/s12325-019-0885-3>
- [48] S. Behring and A. Gonzalez (reviewed by), Healthline. *What Are the Stages of Chronic Venous Insufficiency?* 10.Jun.2021. [Online]. Available from: <https://www.healthline.com/health/chronic-venous-insufficiency-stages> [retrieved: May, 2023]
- [49] N. Kahraman et al., "Detection of Residual Varicose Veins with Near Infrared Light in the Early Period After Varicose Surgery and Near Infrared Light Assisted Sclerotherapy", *Vascular*, vol. 30(6), Oct. 2021. <https://doi.org/10.1177/17085381211051489>
- [50] Cambridge Dictionary. *Artificial Intelligence*. [Online]. Available from: <https://dictionary.cambridge.org/dictionary/english/artificial-intelligence> [retrieved: May, 2023]
- [51] O. Campesato, *Artificial Intelligence, Machine Learning, and Deep Learning*. Mercury Learning and Information, 2020.

- [52] A. Govindu and S. Palwe, "Early Detection of Parkinson's Disease Using Machine Learning", *Procedia Computer Science*, vol. 218, pp. 249-261, Jan. 2023. <https://doi.org/10.1016/j.procs.2023.01.007>
- [53] N. N. Sakhare, I. S. Shaik, and S. Saha, "Prediction of Stock Market Movement via Technical Analysis of Stock Data Stored on Blockchain Using Novel History Bits Based Machine Learning Algorithm", *The Institution of Engineering and Technology IET Software*, Jan. 2023. <https://doi.org/10.1049/sfw2.12092>
- [54] I. Erdem, "Ülkemizdeki Havalimanlarının Yolcu ve Uçak Taleplerinin Çok Yönlü Değerlendirilmesi (Multivariate Analysis of Passenger and Aircraft Demands of Airports in Turkey)", Master's Degree Thesis, Dokuz Eylül University, İzmir, Turkey, Aug. 2012. Thesis in Turkish with an abstract in English. https://tez.yok.gov.tr/UlusalTezMerkezi/tezDetay.jsp?id=beo_mkTrj0BSyzbqajYaYpQ&no=WHgKOWHTcFfbOi8a3PerJA
- [55] Y. LeCun, Y. Bengio, and G. Hinton, "Deep Learning", *Nature*, vol. 521, pp. 436-444, May 2015. <https://doi.org/10.1038/nature14539>
- [56] P. Skalski, Makesense, Alpha. *Free To Use Online Tool For Labelling Photos*. [Online] Available from: <https://www.makesense.ai/> [retrieved: May, 2023]
- [57] T. Mazuryk and M. Gervautz, "History, Applications, Technology And Future", *Virtual Reality Vienna: Vienna University of Technology*, vol.72, 1996. https://www.researchgate.net/publication/2617390_Virtual_Reality_-_History_Applications_Technology_and_Future
- [58] M. A. Gutiérrez, F. Vexo, and D. Thalmann, *Stepping Into Virtual Reality*, England: Springer-Verlag London, 2008. <https://doi.org/10.1007/978-1-84800-117-6>
- [59] W. R. Sherman and A. B. Craig, *Understanding Virtual Reality-Interface, Application and Design*, The United States of America: Morgan Kaufmann Publishers, 2003. <https://doi.org/10.1016/C2013-0-18583-2>
- [60] C. C. Ko and C. D. Cheng, *Interactive web-based virtual reality with Java 3D*. The United States of America: Information Science Reference, 2009.
- [61] H. A. Erdem, "Utilization of Virtual Reality Environment as an Interactive Visual Learning Tool in Primary School Education System", Master's Degree Thesis, Dokuz Eylül University, İzmir, Turkey, Aug. 2013. https://tez.yok.gov.tr/UlusalTezMerkezi/tezDetay.jsp?id=iofm_MFGdK7U1KPrXLYjzQ&no=L77dJQmcOK5zBMOxhpMçUw
- [62] P. Milgram, H. Takemura, A. Utsumi, and F. Kishino, "Augmented Reality: A Class of Displays on the Reality-Virtuality Continuum", *Telemanipulator and Telepresence Technologies. Society of Photo-Optical Instrumentation Engineers (SPIE) Digital Library*, vol. 2351, pp. 282-292, Dec. 1995. <https://doi.org/10.1117/12.197321>
- [63] J. B. Alves, B. Marques, C. Ferreira, P. Dias, and B. S. Santos, "Comparing Augmented Reality Visualization Methods for Assembly Procedures", *Virtual Reality*, vol. 26, pp. 235-248, Jul. 2022. <https://doi.org/10.1007/s10055-021-00557-8>